J Low Temp Phys (2008) 151: 635–639
DOI 10.1007/s10909-008-9727-4

Operation of an X-ray Transition-Edge Sensor Cooled by Tunnel Junction Refrigerators

N.A. Miller · J.A. Beall · G.C. Hilton · K.D. Irwin · G.C. O'Neil · D.R. Schmidt · L.R. Vale · J.N. Ullom

Received: 23 July 2007 / Accepted: 9 October 2007 / Published online: 19 January 2008

Abstract We demonstrate successful cooling of an X-ray transition-edge sensor (TES) using solid-state refrigerators based on normal-metal/insulator/superconductor (NIS) tunnel junctions. Above the TES transition temperature (T_c), we use Johnson-noise thermometry to measure the cooling performance. In this regime, the NIS refrigerators cool the TES from 300 mK to 220 mK and from 220 mK to $T_c = 160$ mK. Below T_c, we also observe cooling and demonstrate that the operation of the NIS refrigerators introduces no detectable noise into the TES readout.

Keywords NIS junction · Refrigeration · TES · Tunneling · X-ray detector

PACS 07.20.Mc · 85.25.Oj · 85.25.-j · 85.25.Am · 85.30.Mn

Transition-edge sensors (TESs) are an important technology for high-resolution X-ray spectroscopy, especially for applications in materials analysis and X-ray astronomy [1, 2]. TES detectors are superconducting thin-films typically operated near 100 mK for optimal performance. Traditional refrigerators used to reach 100 mK temperatures, adiabatic demagnetization refrigerators (ADRs) and dilution refrigerators, can be impractical for some applications due to their expense, size, and/or weight. Examples include commercial X-ray microanalysis systems, where cost and size are issues, and space-borne detectors, where size and weight are of concern. Normal-metal/insulator/superconductor (NIS) tunnel junctions are an alternative refrigeration technology, with the potential to cool from 300 mK to 100 mK [3, 4]. Operation of an

N.A. Miller (✉) · J.A. Beall · G.C. Hilton · K.D. Irwin · G.C. O'Neil · D.R. Schmidt · L.R. Vale · J.N. Ullom
National Institute of Standards and Technology, Boulder, CO 80305, USA
e-mail: nmiller@boulder.nist.gov

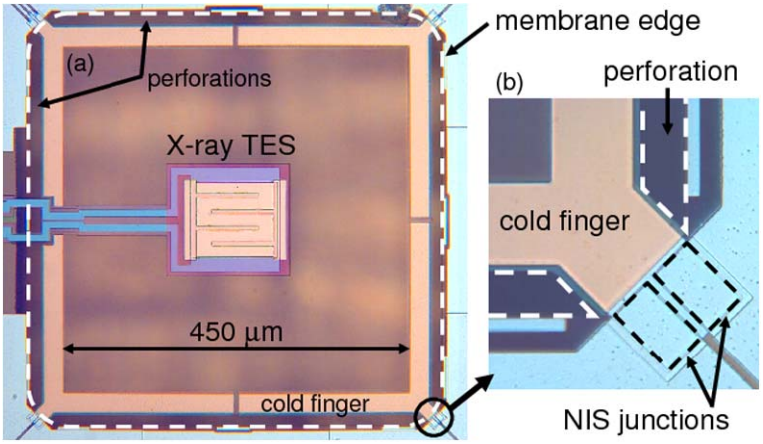

Fig. 1 (Color online.) (**a**) TES X-ray sensor integrated with NIS refrigerators. Four pairs of NIS junctions, each 7 µm by 10 µm, are located on the bulk substrate at the corners of a micro-machined SiNx membrane (*dashed white outline*). Y-shaped normal-metal cold fingers extend from the refrigerator junctions onto the membrane and surround the TES. A 100 µm-square TES X-ray sensor is located in the center of the membrane. (**b**) Magnified view of membrane corner. The membrane is perforated between the membrane edge and the cold fingers (*dashed white outline*)

NIS junction removes the hottest electrons from the normal-metal by quantum mechanical tunneling. Combining NIS refrigerators with a sorption-pumped ^{3}He system, which is relatively cheap and small, would provide a third option for cooling devices to 100 mK, and could make TES detectors more accessible. Alternatively, combining NIS refrigerators with an ADR could allow for more design options, including extended hold times, reduced mass, or lower stray magnetic fields from the ADR.

An X-ray TES cooled by NIS refrigerators is shown in Fig. 1. The TES consists of a 100 µm-square bilayer of Mo and Cu, with a transition temperature $T_c \sim 159$ mK and a normal-state resistance $R_{n,\mathrm{TES}} \sim 8$ mΩ. Four normal-metal Cu bars are added to reduce "excess noise" [5]. The TES is voltage biased, with a shunt resistor $R_{sh} = 118$ µΩ, and read out by two stages of superconducting quantum interference devices (SQUIDs).

The TES is suspended on a low-stress SiNx membrane, 0.5 µm-thick and 500 µm-square. The membrane is perforated along the edges to limit the thermal conductance to the substrate. The resulting membrane is connected to the substrate through four 23 µm-wide corner legs and two 14 µm-wide side legs for the TES wiring.

A pair of NIS refrigerator junctions, each 7 µm-wide by 10 µm-long, is placed at each corner of the membrane. The refrigerators are located on the bulk substrate, with measured normal state resistance $R_{n,\mathrm{NIS}} = 252$ Ω and measured junction resistance at zero bias $R_d \sim 500$ kΩ (for eight junctions in series). A normal-metal cold finger extends from each junction pair onto the membrane to completely surround the TES. Details of the NIS membrane cooling mechanism are described elsewhere [6].

The device in Fig. 1 was cooled in an ADR to temperatures T_{ADR} of 50 mK to 400 mK. Current-voltage (I–V) curves of the NIS refrigerator are diode-like, with a current onset at a voltage set by the effective energy gap. The effective gap of

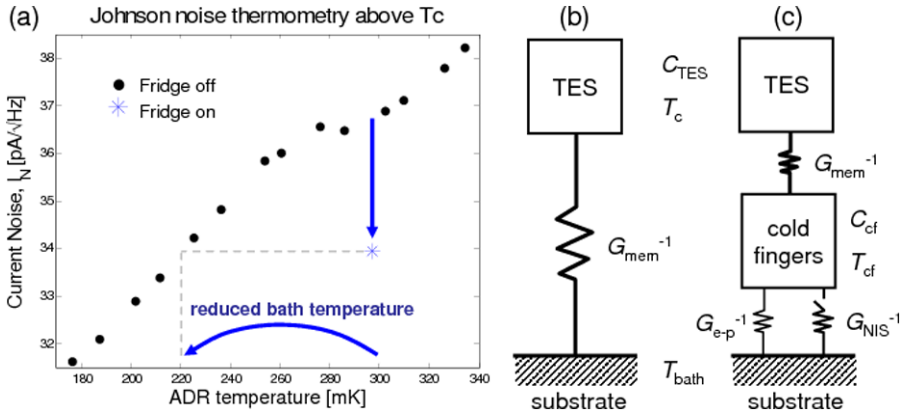

Fig. 2 (Color online.) (**a**) TES current noise I_N (averaged from 1–10 kHz) vs. ADR temperature. I_N with NIS refrigerators off (*black dots*) is used as a temperature calibration. Cooling from an ADR temperature of 300 mK (*blue star*) reduces the current noise, corresponding to a reduced bath temperature of 220 mK. (**b**) Simple thermal model used for traditional TES detectors. (**c**) Thermal model for NIS-cooled X-ray TES. Heat capacities C, thermal conductances G, and temperatures T are labeled for each element. In both (**b**) & (**c**), G_{ETF} has been omitted for clarity

eight junctions in series is eight times the superconducting gap energy Δ, where $\Delta = 189$ μeV for our Al. We observed a maximum reduction in membrane temperature at a refrigerator voltage bias $V_b = 0.91 * \Delta/e$, consistent with theory [4].

At temperatures above T_c, the TES is resistive and Johnson-noise thermometry can be used to measure the membrane cooling due to the NIS refrigerator. Current noise I_N is measured using a signal analyzer, and the average noise between 1–10 kHz is plotted in Fig. 2a. The current noise is

$$I_N = \sqrt{I_{N,\mathrm{sys}} + \frac{4 k_B T}{R}}, \tag{1}$$

where $I_{N,\mathrm{sys}}$ is the system noise due to the SQUIDs (previously measured to be $10\ pA/\sqrt{Hz}$), k_B is the Boltzmann constant, T is the temperature of the TES, and R is the total resistance ($R_{n,\mathrm{TES}} + R_{sh}$). When the NIS junctions are unbiased (off), T is equal to T_{ADR} and the measured I_N vs. T_{ADR} curve can be used as a temperature calibration. Biasing the NIS refrigerators reduces the temperature of the cold fingers on the membrane, thus providing a lower effective bath temperature for the TES, which reduces the current noise. Figure 2a shows that for an ADR temperature of 300 mK, biasing the refrigerators cools the TES to 220 mK. For ADR temperatures below 220 mK, the TES is cooled below $T_c = 160$ mK and Johnson-noise thermometry can no longer be used to quantify cooling.

At temperatures below T_c, the change in the TES I–V curves with the NIS refrigerators on and off must be used to measure cooling. However, quantifying cooling from the I–V curves is potentially complicated because operation of the NIS refrigerators can change the total thermal conductance between the TES and the substrate (G_{tot}). As shown in Fig. 2c, the addition of the NIS refrigerators and cold fingers makes the thermal model more complicated compared to a traditional TES model

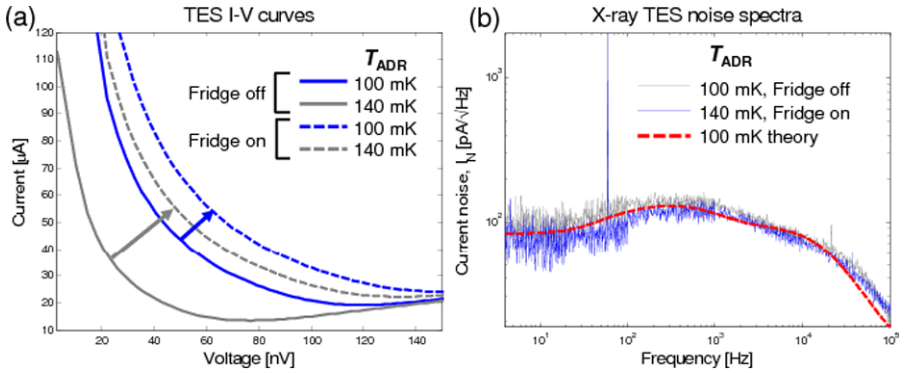

Fig. 3 (Color online.) (**a**) TES I–V curves at two ADR temperatures, with the NIS refrigerators on and off. The NIS cooling performance cannot be read off the graph due to changes in the total thermal conductance when the NIS refrigerators are turned on. (**b**) Current noise spectra of the TES biased at 25% Rn (bias power ∼1 pW). The peak at 300 Hz is due to the additional cold finger heat capacity (Fig. 2c). The theory curve is generated for an uncooled TES, using an "excess noise" factor of $M = 0.82$. ADR temperatures of 100 mK and 140 mK were chosen to compare similar membrane bath temperatures based on estimated NIS cooling

(Fig. 2b). When the NIS refrigerators are off, the thermal conductance between the cold fingers and substrate is set by the electron-phonon coupling in the normal-metal of the NIS junctions (G_{e-p}). Biasing the NIS refrigerators adds an additional thermal conductance due to the power removed from the normal-metal electrons ($P_{\rm cool}$), defined as $G_{\rm NIS} = dP_{\rm cool}/dT$ (similar to the additional thermal conductance $G_{\rm ETF}$ due to electrothermal feedback of the TES).

In the limit where the membrane thermal conductance ($G_{\rm mem}$) is much lower than either G_{e-p} or $G_{\rm NIS}$, the thermal model simplifies to the traditional TES model (Fig. 2b), where the cold finger takes the place of the substrate. This is the case for previous work using NIS refrigerators to cool a TES mm-wave detector where the membrane legs are extremely long and thin [7, 8]. In this limiting case, $G_{\rm tot}$ is approximately the same with the NIS refrigerators on and off. Therefore, cooling can be quantified by matching cooled TES I–V curves with the corresponding uncooled curves.

For the X-ray devices discussed here, TES I–V curves with the refrigerators on and off are shown in Fig. 3a. The temperature reduction cannot be simply read off the plot because $G_{\rm tot}$ changes when the NIS refrigerators are turned on, unlike the limiting case discussed above. As a result, the full thermal model (Fig. 2c) must be used to quantify cooling of the X-ray TES below T_c. The ability of the NIS refrigerators to cool the biased TES through the transition provides evidence of cooling below T_c. However, we are presently unable to quantify the cooling, due to limits in our knowledge of the numerous thermal conductances in the device. We are presently fabricating test devices that will allow us to directly measure $G_{\rm mem}$. Other test devices will include a Johnson-noise thermometer directly on a cold finger. With these additional devices, we will be able to directly measure the temperature of the cold fingers and test the validity of our thermal model.

The cooling performance of the current NIS refrigerators is significantly below the theoretical limit (300 mK to 100 mK), suggesting much room for improvement. The performance is limited by unnecessarily thick tunnel barriers and the return of $\sim 4\%$ of the power deposited in the superconductor. We have previously fabricated thinner tunnel junctions and the power return can be decreased by improving the design of the quasi-particle traps.

In addition to cooling performance, it is also important that the NIS refrigerators do not degrade the noise performance of the TES detector. The current noise of the TES is shown in Fig. 3b, with the NIS refrigerators on and off. Operation of the NIS refrigerators adds no measurable noise to the TES noise spectra. The noise theory curve was generated from the multi-element thermal model in Fig. 2c [9]. The slight bump in the noise near 300 Hz is due to the addition of the cold finger heat capacity. That the theory curve also exhibits the same noise bump leads us to believe that our thermal model is a good approximation.

A similar device was fabricated with an additional 1.6 μm-thick Bi absorber attached to the TES to increase X-ray absorption. With this device, we have observed 6 keV X-ray pulses. However, we were unable to obtain an energy spectrum because the X-rays saturated the TES, driving it into its normal-resistance state. Devices presently in fabrication have larger TES detectors to increase the saturation energy.

In conclusion, we have demonstrated successful NIS refrigeration of an X-ray TES. Above T_c, the NIS refrigerators cooled the TES from 300 mK to 220 mK and from 220 mK to 160 mK. Below T_c, the cooling cannot be quantified with the present measurements. The operation of the NIS refrigerators introduces no measurable noise to the TES noise spectra. We are presently making new devices to further explore NIS-cooled X-ray TES operation. Diagnostic devices with additional noise thermometers on a cold finger and in place of the X-ray TES will allow for a complete determination of cooling performance at all temperatures.

References

1. D.A. Wollman, K.D. Irwin, G.C. Hilton, L.L. Dulcie, D.E. Newbury, J.M. Martinis, J. Microsc. **188**, 196 (1997)
2. F.S. Porter, Nucl. Instrum. Methods Phys. Res. A **520**, 354 (2004)
3. M. Nahum, T.M. Eiles, J.M. Martinis, Appl. Phys. Lett. **65**, 3123 (1994)
4. A.M. Clark, A. Williams, S.T. Ruggiero, M.L. van den Berg, J.N. Ullom, Appl. Phys. Lett. **84**, 625 (2004)
5. J.N. Ullom, W.B. Doriese, G.C. Hilton, J.A. Beall, S. Deiker, W.D. Duncan, L. Ferreira, K.D. Irwin, C.D. Reintsema, L.R. Vale, Appl. Phys. Lett. **84**, 4206 (2004)
6. N.A. Miller, A.M. Clark, A. Williams, S.T. Ruggiero, G.C. Hilton, J.A. Beall, K.D. Irwin, L.R. Vale, J.N. Ullom, IEEE Trans. Appl. Supercond. **15**, 556 (2005)
7. R.F. Silverberg, D.J. Benford, T.C. Chen, J. Chervenak, F. Finkbeiner, S.H. Moseley, W.D. Duncan, N.A. Miller, D.R. Schmidt, J.N. Ullom, Nucl. Instrum. Methods Phys. Res. A **559**, 630 (2006)
8. R.F. Silverberg, D.J. Benford, T.C. Chen, J. Chervenak, F. Finkbeiner, N.A. Miller, D.R. Schmidt, J.N. Ullom, J. Low Temp. Phys., these proceedings
9. J.M. Gildemeister, Voltage-biased superconducting bolometers for infrared and mm-waves. Ph.D. thesis, UC Berkeley, 2000